

Extremely Hot Late-Summer Conditions in Northern and Eastern Japan in 2012

16 November 2012

Tokyo Climate Center, Japan Meteorological Agency

Northern and eastern Japan experienced extremely high temperatures in the late summer of 2012 due to the significantly enhanced North Pacific High to the east of the country. Record-high temperatures were set over northern Japan for three consecutive 10-day periods* from late August to mid-September. The 10-day mean sea surface temperature (SST) averaged over the area around northern Japan for mid-September was the highest on record for all 10-day periods of the year since 1985.

* Note: There are three 10-day periods in each month, making a total of thirty-six in a year. The third nominal 10-day period of each month may not in fact have only 10 days (e.g., the third 10-day period of August covers 11 days from the 21st to 31st).

1. Surface climate conditions

In northern and eastern Japan, hot sunny conditions prevailed from mid-August to mid-September, and temperatures remained significantly above normal for this time of the year (Figure 17). For example, Sapporo City in northern Japan's Hokkaido region experienced very hot conditions every day from late August to mid-September, and daily mean temperatures persisted above the annual high of the climatological normal (Figure 18).

The values of 10-day mean temperatures averaged over northern Japan were the highest on record for three consecutive 10-day periods from late August to mid-September (Table 3). Those for eastern Japan were the second highest on record for late August and early September, and the value for mid-September tied the record-high set in 2011. Collection of 10-day mean temperature records for divisions of Japan began in 1961.

Table 3 Top three 10-day mean temperature anomalies (unit: °C) averaged over northern and eastern Japan from late August to mid-September

Collection of statistical records began in 1961. Anomalies are deviations from the 1981 – 2010 average, and the figures in red denote records for 2012.

Northern Japan	Highest	2nd highest	3rd highest
21 – 31 August	+3.5 (2012)	+3.1 (2010)	+1.9 (2000)
1 – 10 September	+3.3 (2012)	+3.1 (2010)	+2.5 (2011)
11 – 20 September	+5.5 (2012)	+2.0 (2000)	+1.8 (2007)

Eastern Japan	Highest	2nd highest	3rd highest
21 – 31 August	+2.7 (2010)	+2.1 (2012)	+1.7 (2000)
1 – 10 September	+2.9 (2010)	+1.5 (2012)	+1.5 (1961)
11 – 20 September	+3.1 (2012)	+3.1 (2011)	+2.3 (2003)

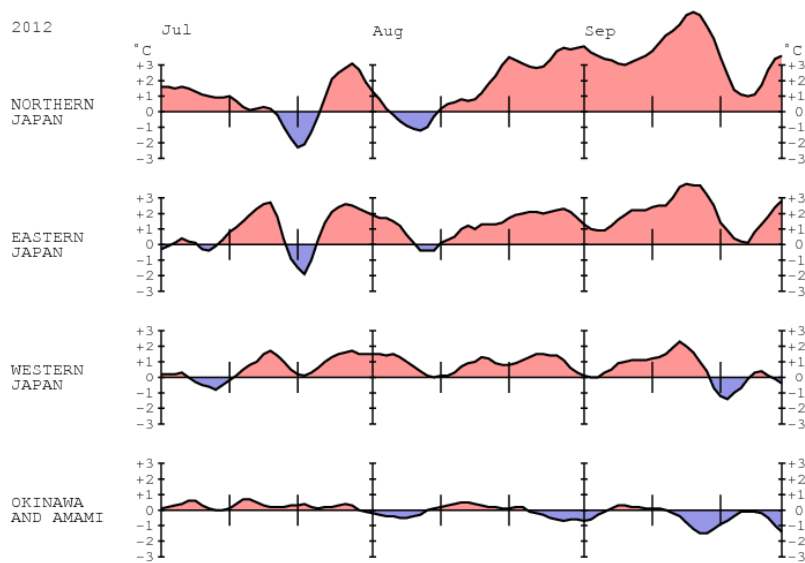


Figure 17 Time-series representation of five-day running mean temperature anomalies (unit: °C) for four divisions of Japan from 1 July to 30 September, 2012
Anomalies are deviations from the 1981 – 2010 average.

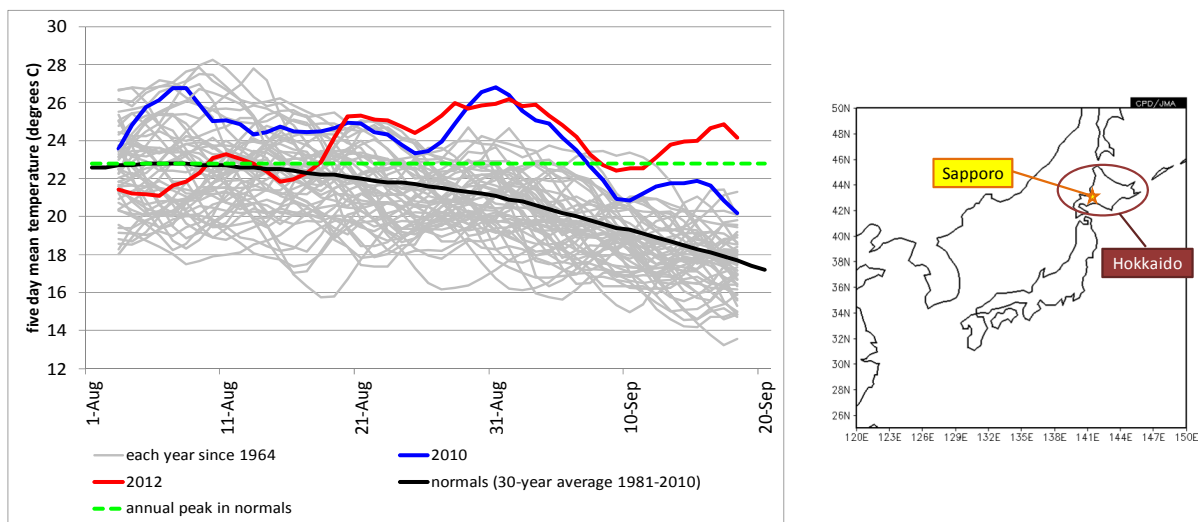


Figure 18 Time-series representation of five-day running mean temperatures in Sapporo from 3 August to 18 September between 1961 and 2012

The red and blue lines indicate values for 2012 and 2010 (the previous record for high temperatures in late summer), respectively. Green denotes the highest value among daily mean temperatures in the climatological normal (i.e., the 1981 – 2010 average) for Sapporo.

2. Characteristic atmospheric circulation causing Japan’s hot late-summer conditions

The significantly enhanced Pacific High to the east of Japan persisted from late August to mid-September 2012 (Figures 19 and 20 (a)). Northern and eastern Japan experienced extremely high temperatures due to southerly warm-air advection and sunny conditions (i.e., above-normal amounts of solar radiation) attributed to the northward extension of this high.

The Pacific High to the east of Japan in late August – mid-September was at its strongest for this time of the year since 1979 (Figure 20 (b)). The westerly jet stream in the upper troposphere

showed significant northward meandering near Japan (Figure 21) in line with prominent anticyclonic circulation anomalies centered over the area to the northeast of the country (Figure 22). In association, negative anomalies of potential vorticity (PV) in the upper troposphere were centered northeast of Japan (Figure 23). The enhanced anticyclone east of the country featured an equivalent barotropic structure and a warm air mass, and its vertical axis exhibited a slight northward tilt with height (Figure 24). It is presumed that upper-level PV anomalies induced the enhanced equivalent-barotropic anticyclone (Hoskins et al. 1985).

In the upper troposphere, wave trains were seen along the Asian jet stream in association with the eastward propagation of Rossby wave packets (Figure 25). Convective activity associated with the Asian summer monsoon was enhanced over the Arabian Sea, Pakistan, India and the Bay of Bengal (Figure 26). According to statistical analysis, when convective activity is enhanced over these areas in and around South Asia from late August to mid-September, wave trains with anticyclonic circulation anomalies north of Japan tend to appear along the Asian jet stream (Figure 27) as seen in 2012 (Figure 25). These trains are similar to those of the Silk Road pattern highlighted by T. Enomoto (Enomoto et al. 2003; Enomoto 2004). It can be presumed from the results of statistical analysis and research performed to date that active convection associated with monsoon activity in and around South Asia contributed to the development of the enhanced anticyclone near Japan through the eastward propagation of quasi-stationary Rossby wave packets along the Asian jet.

In late August and mid-September 2012, convective activity was enhanced northeast of the Philippines (Figure 26); several typhoons formed in the area, moving northward over Okinawa (southwestern Japan) and the South China Sea (Figure 28). According to statistical analysis, wave trains tend to appear in the area from the Philippines to Japan and the northern Pacific in association with the variability of convective activity northeast of the Philippines from late August to mid-September (Figure 29). This teleconnection formation is called the Pacific-Japan (PJ) pattern (Nitta 1986; 1987). The outcomes of statistical analysis and research performed to date indicate that active convection northeast of the Philippines and typhoons contributed to the strength of the Pacific High over northern and eastern Japan.

The possible primary factors contributing to Japan's hot late-summer conditions are summarized in Figure 30, but the related mechanisms have not yet been fully clarified.

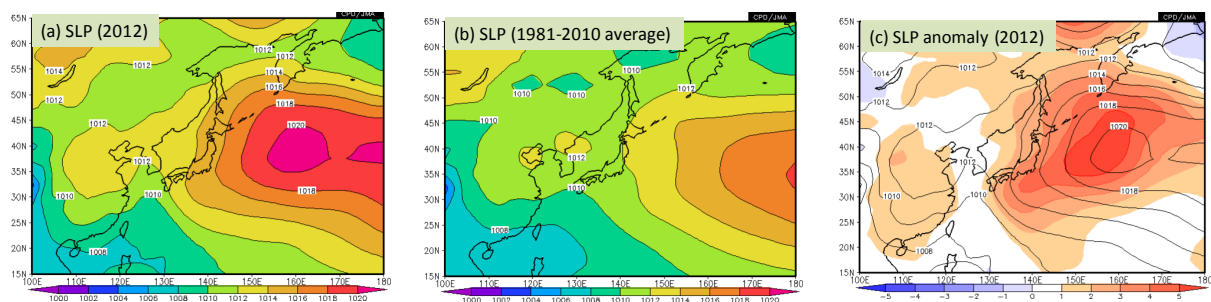


Figure 19 Sea level pressure (SLP) averaged from 21 August to 20 September for (a) 2012, (b) the normal (i.e., the 1981 – 2010 average) and (c) 2012 and anomalies (i.e., deviations from the normal) The contour interval is 2 hPa.

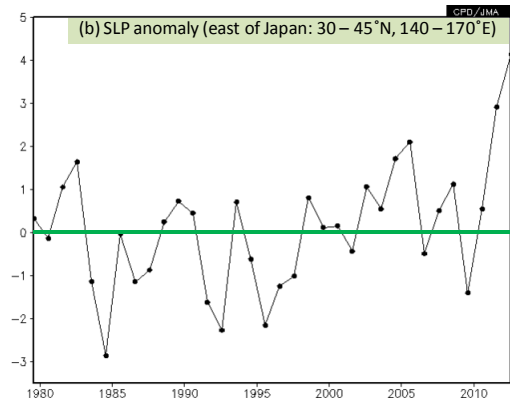
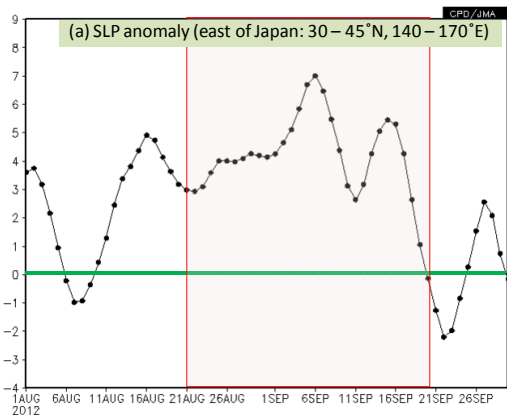


Figure 20 (a) Time-series representation of five-day running mean values of SLP anomalies (unit: hPa) averaged over the area east of Japan (30°N – 45°N, 140°E – 170°E) from 1 August to 30 September, 2012, and (b) interannual variability of area-mean SLP anomalies averaged between 21 August and 20 September from 1979 to 2012

Anomalies are deviations from the 1981 – 2010 average. The red rectangle in the panel on the left shows the period from 21 August to 20 September, 2012.

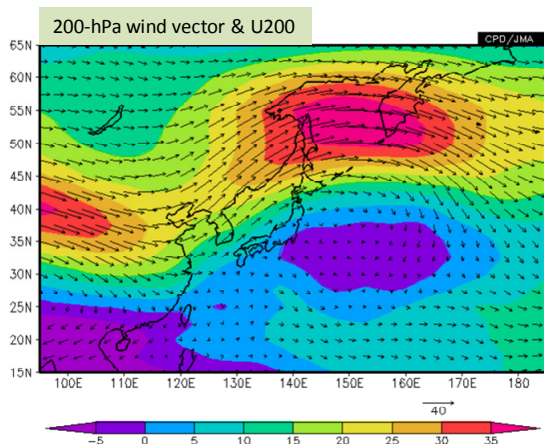


Figure 21 200-hPa wind vectors and zonal wind speeds averaged from 21 August to 20 September, 2012

The shading shows zonal wind speeds (unit: m/s).

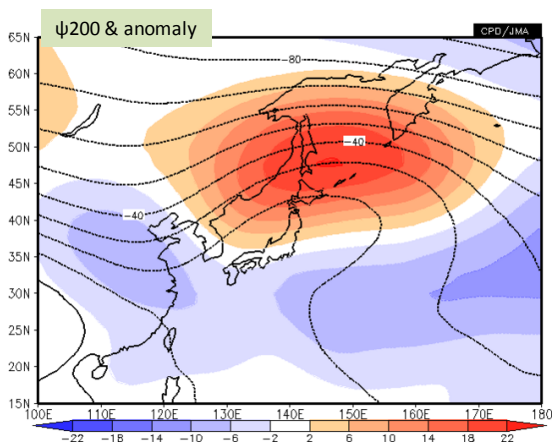


Figure 22 200-hPa stream function (contours) and anomalies (shading) averaged from 21 August to 20 September, 2012

The contour interval is 10^6 m²/s. Positive (warm color) and negative (cold color) stream function anomalies in the Northern Hemisphere indicate anticyclonic and cyclonic circulation anomalies. Anomalies are deviations from the 1981 – 2010 average.

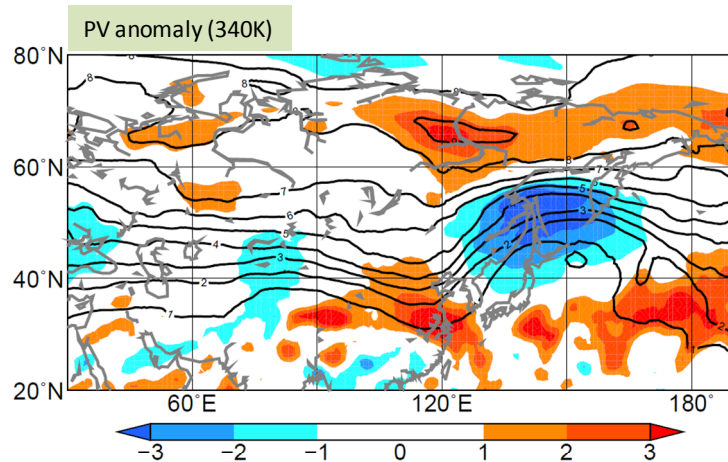


Figure 23 Potential vorticity on the 340 K isentropic surface (contours; unit: s^{-1}) and normalized anomalies (shading) averaged from 21 August to 20 September, 2012

Anomalies (i.e., deviations from the 1981 – 2010 average) are normalized by their standard deviations.

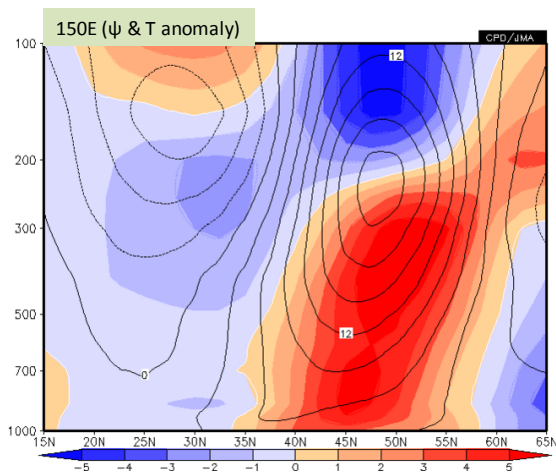


Figure 24 The vertical-meridional section of stream function anomalies (contours; unit: $10^6 m^2/s$) and temperature anomalies (shading; unit: $^{\circ}C$) averaged from 21 August to 20 September, 2012, along the $150^{\circ}E$ meridian

Anomalies are deviations from the 1981 – 2010 average.

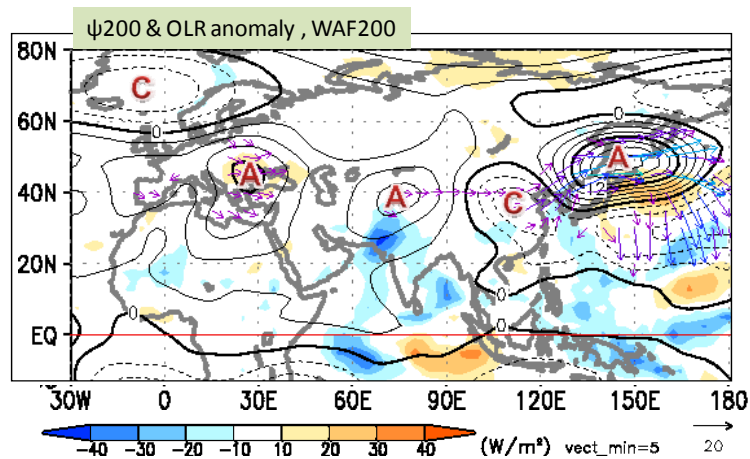


Figure 25 200-hPa stream function anomalies (contours), 200-hPa wave activity flux (vectors; unit: m^2/s^2), and outgoing longwave radiation (OLR) anomalies averaged from 21 August to 20 September, 2012

“A” and “C” indicate the centers of anticyclonic and cyclonic circulation anomalies, respectively. The contour interval is $3 \times 10^6 m^2/s$. Negative (cold color) and positive (warm color) OLR anomalies (unit: W/m^2) show enhanced and suppressed convection, respectively. Anomalies are deviations from the 1981 – 2010 average. The wave activity flux is calculated after Takaya and Nakamura (2001).

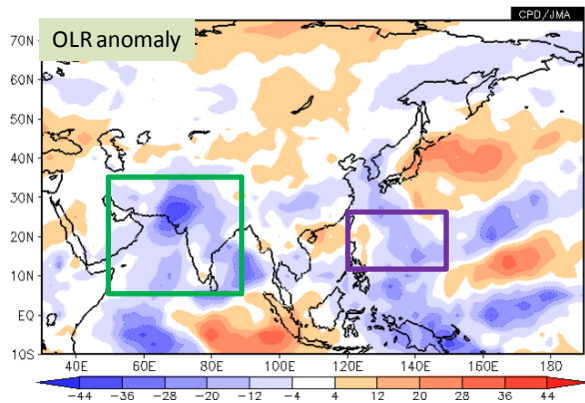


Figure 26 OLR anomalies averaged from 21 August to 20 September, 2012

The green and purple rectangles indicate the area around South Asia ($5^{\circ}\text{N} - 35^{\circ}\text{N}$, $50^{\circ}\text{E} - 90^{\circ}\text{E}$) and the area northeast of the Philippines ($10^{\circ}\text{N} - 25^{\circ}\text{N}$, $120^{\circ}\text{E} - 150^{\circ}\text{E}$), respectively. Anomalies are deviations from the 1981 – 2010 average.

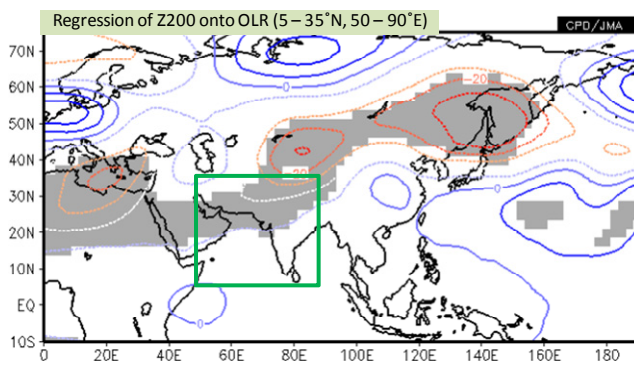


Figure 27 200-hPa geopotential height (contours; unit: m) regressed onto a time-series representation of area-averaged OLR values in and around South Asia (green rectangle: $5^{\circ}\text{N} - 35^{\circ}\text{N}$, $50^{\circ}\text{E} - 90^{\circ}\text{E}$) for the period from 21 August to 20 September, 2012

The contour interval is 5 m. The gray shading indicates a 95% confidence level. The base period for the statistical analysis is 1979 – 2011.

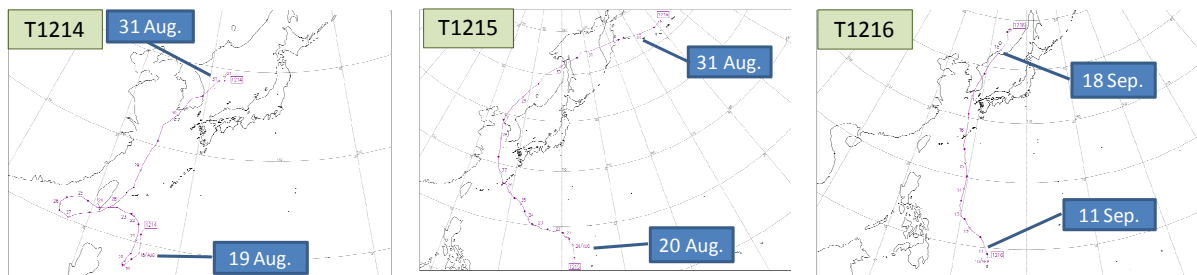


Figure 28 Typhoons forming from late August to mid-September 2012

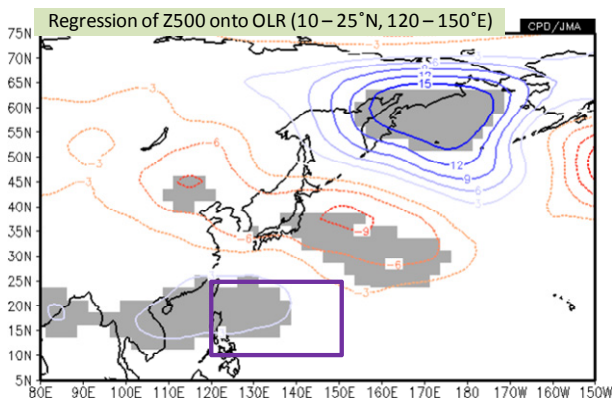


Figure 29 500-hPa geopotential height (contours; unit: m) regressed onto a time-series representation of area-averaged OLR values for the area northeast of the Philippines (purple rectangle: $10^{\circ}\text{N} - 25^{\circ}\text{N}$, $120^{\circ}\text{E} - 150^{\circ}\text{E}$) covering the period from 21 August to 20 September

The contour interval is 3 m. The gray shading indicates a 95% confidence level. The base period for the statistical analysis is 1979 – 2011.

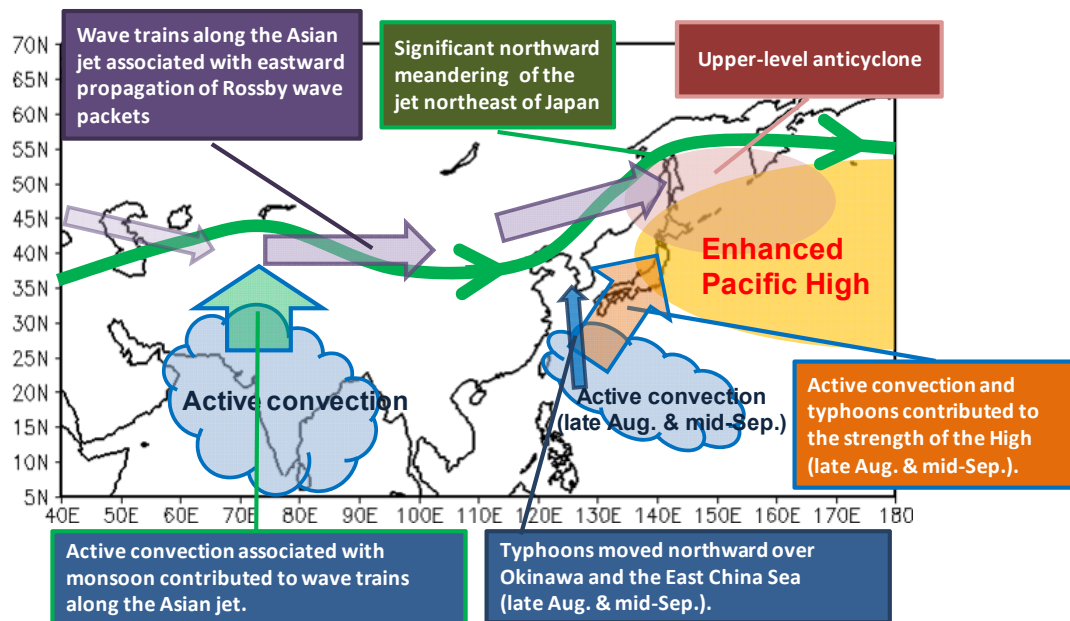


Figure 30 Primary factors contributing to the hot late-summer conditions of 2012 in northern and eastern Japan

3. Sea surface temperatures around northern Japan

Sea surface temperatures (SSTs) around northern Japan were significantly higher than normal (i.e., the 1981 – 2010 average) from late August to mid-September 2012 (Figure 31). The value of 10-day mean SSTs averaged for the area around Hokkaido (the white rectangle in Figure 31) for mid-September 2012 was 22.5°C (preliminary), which was 4.6°C above normal (Table 4) and exceeded the previous record of 21.4°C set in late August 2010 for all 10-day periods of the year since 1985. In the normal, SSTs in the area reach annual maximum levels in August and September. The values of area-averaged SSTs for the two consecutive 10-day periods of early and mid-September 2012 were the highest on record for the respective periods of the year since 1985 (Table 4; Figure 32).

In the seas around Hokkaido, surface seawater was warmer than normal due to predominant sunny conditions (i.e., above-normal amounts of solar radiation) associated with the enhanced North Pacific High that caused record-breaking high temperatures in northern Japan. In addition, near-surface seawater was less mixed with cold seawater below it by surface winds, and ocean heat accumulated between the surface and just above 10 m in depth due to calm conditions associated with the enhanced Pacific High (Figure 33). The record-high SSTs observed around Hokkaido can be attributed to these factors relating to the enhanced North Pacific High east of Japan.

Table 4 Record-high (preliminary) 10-day mean SSTs (unit: °C) averaged over the area around Hokkaido in northern Japan for early and mid-September

The SST values for September 2012 are preliminary. Collection of statistical records began in 1985, since when SST statistics have been based on satellite observations in addition to ship observations. Anomalies are deviations from the 1981 – 2010 average. The area for the average is the white rectangle shown in Figure 31.

Seas around Hokkaido	Area-averaged SSTs	Anomalies	Previous record high
1 – 10 September	21.8	+3.3	21.1 (2010)
11 – 20 September	22.5	+4.6	20.1 (1999)

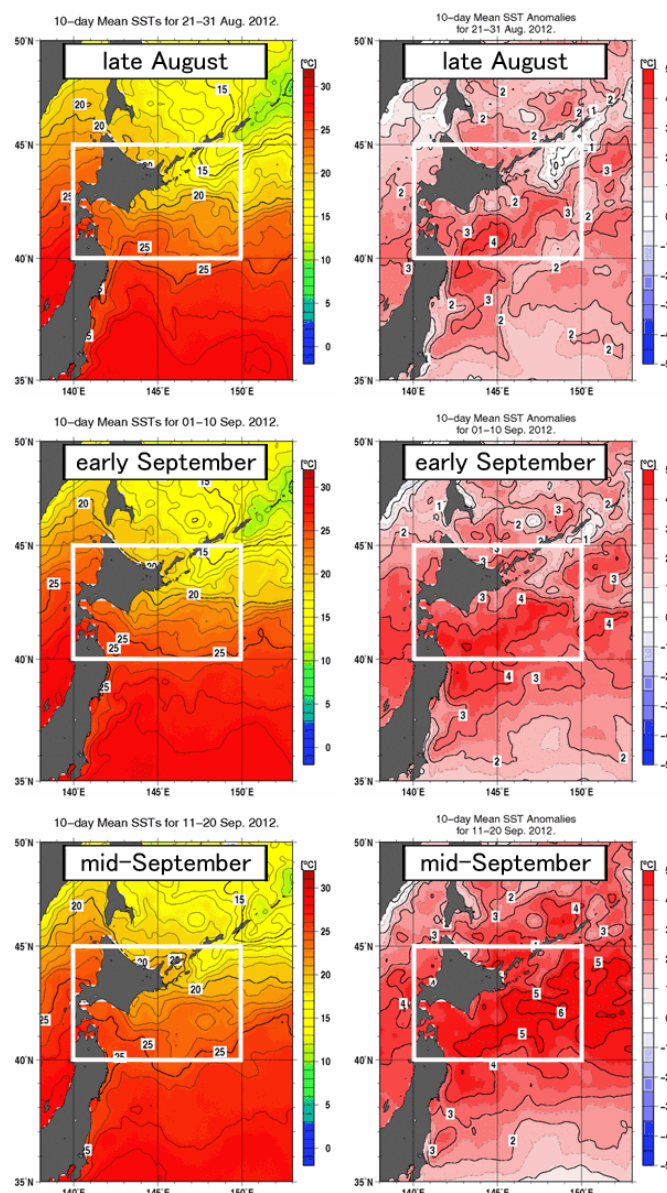


Figure 31 10-day mean SSTs (left) and anomalies (right) for late August (top), early September (middle) and mid-September 2012 (bottom)

Anomalies are deviations from the 1981 – 2010 average, and the unit for SSTs and anomalies is °C. The white rectangle indicates the target area around Hokkaido.

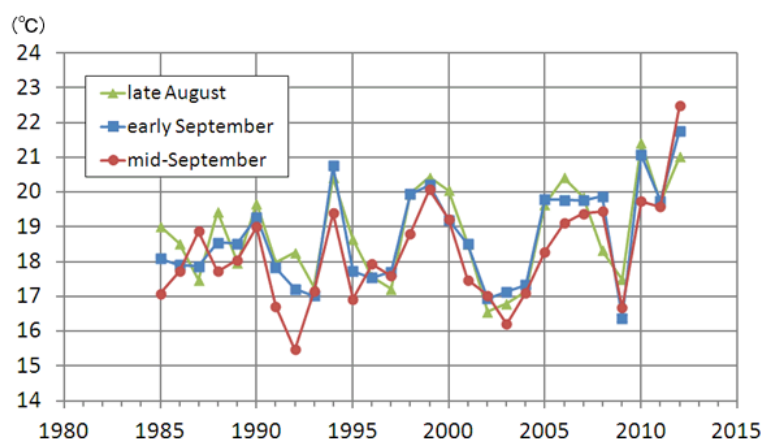


Figure 32 Interannual variability of 10-day mean SSTs averaged over the area around Hokkaido (white rectangle shown in Figure 31) for late August (green line), early September (blue line) and mid-September (red line) from 1985 to 2012

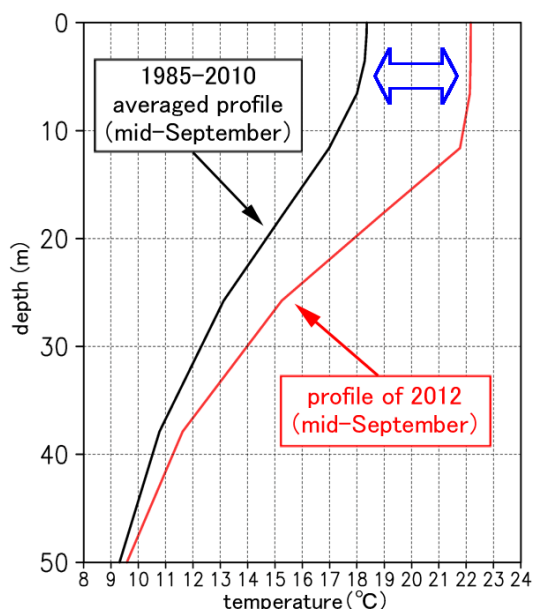


Figure 33 Temperature profile for seawater between the surface and a depth of 50 m averaged over the area around Hokkaido (white rectangle shown in Figure 31) for mid-September of 2012 (red line) and the 1985 – 2010 average (black line)

Deviations from the 1985 – 2010 average were significant between the surface and just above 10 m in depth, and were small at 50 m in depth.

References

- Enomoto, T., B. J. Hoskins, and Y. Matsuda, 2003: The formation mechanism of the Bonin high in August, *Quart J. Roy. Meteor. Soc.*, **587**, 157-178.
- Enomoto, T., 2004: Interannual variability of the Bonin high associated with the propagation of Rossby waves along the Asian jet. *J. Meteor. Soc. Japan*, **82**, 1019-1034.
- Hoskins, B., M. E. McIntyre, and A. W. Robertson, 1985: On the use and significance of isentropic potential vorticity maps, *Quart J. Roy. Meteor. Soc.*, **111**, 877-946.
- Nitta, T., 1986: Long-term variations of cloud amount in the western Pacific region. *J. Meteor. Soc. Japan*, **64**, 373-390.
- Nitta, T., 1987: Convective activities in the tropical western Pacific and their impact on the Northern Hemisphere summer circulation. *J. Meteor. Soc. Japan*, **65**, 373-390.
- Takaya, K., and H. Nakamura, 2001: A formulation of a phase-independent wave-activity flux for stationary and migratory quasigeostrophic eddies on a zonally varying basic flow. *J. Atom. Sci.*, **58**, 608 – 627.